Available online at www.sciencedirect.com

ScienceDirect

Advances in Space Research 74 (2024) 2376–2387

ADVANCES IN SPACE RESEARCH (a COSPAR publication)

www.elsevier.com/locate/asr

GEO satellite on-orbit refueling and debris removal hybrid mission planning under uncertainty

Weikui Liang [a,b], Hui Zhi [c], Peng Han [a,d], Guangtao Ran [a,*], Guangfu Ma [a], Yanning Guo [a]

[a] Department of Control Science and Engineering, Harbin Institute of Technology, Harbin 150001, China
[b] Aerospace System Engineering, Shanghai 201109, China
[c] Department of Mechanical Engineering, The Hong Kong Polytechnic University, Hong Kong Special Administrative Region
[d] Department of Industrial and Systems Engineering, The Hong Kong Polytechnic University, Hong Kong Special Administrative Region

Received 29 January 2024; received in revised form 1 May 2024; accepted 24 May 2024
Available online 3 June 2024

Abstract

This article proposes two optimization models to solve the multi-satellite on-orbit hybrid service mission planning problem under uncertainty. During the process of on-orbit refueling and debris removal, two categories of uncertainties are taken into account. These uncertainties have an impact on the mass of the service satellite as well as its fuel consumption during the orbit transfer. The two-stage orbit transfer strategy is given to save fuel for maneuvering, which also determines the directed graph between target orbits of satellites or debris. The stochastic expectation model is to get the service sequence with the optimal average benefit, while the robust model considers the worst situation and gives the optimal minimum benefit. Simulations of GEO satellites in orbit are conducted to demonstrate the impact of various models on handling uncertain tasks.

Keywords: Geosynchronous orbit; On-orbit refueling; Debris removal; Multi-satellite; Mission planning; Hybrid uncertainty

1. Introduction

The technology of on-orbit service (OOS), which encompasses on-orbit refueling (Zhang et al., 2014; Meng et al., 2019; Sorenson and Pinkley, 2023), debris removal (Yu et al., 2014; Bang and Ahn, 2019; Li and Baoyin, 2019; Jia et al., 2023), repairing (Han et al., 2019; Han et al., 2022b), and inspection (Zhou et al., 2015a; Peng et al., 2021; He et al., 2023), has seen rapid advancements in recent years. Utilizing OOS technology can substantially extend the lifespan of various satellites, yielding greater economic benefits for space engineering. As a result, many countries and institutions have begun to implement this technology in their prototypes. Such as China's Tianyuan-1 (2016) for on-orbit refueling (Yao, 2016) and the UK's University of Surrey's RemoveDEBRIS mission (2018) (Forshaw et al., 2020; Aglietti et al., 2020).

Currently, most on-orbit refueling missions are in one-to-one mode, while the costs are nearly equivalent to launching a new satellite. For better economic efficiency, service satellites should be capable of providing continuous and cooperative services to multiple client satellites. In fact, the recently launched Mission Extension Vehicle-1/2 (MEV-1/2) by the United States has attempted to extend the lifespan of multiple GEO satellites (Redd, 2020). In

* Corresponding author.
E-mail addresses: hui1225.zhi@connect.polyu.hk (H. Zhi), ranguangtao@hit.edu.cn (G. Ran), magf@hit.edu.cn (G. Ma), guoyn@hit.edu.cn (Y. Guo).

https://doi.org/10.1016/j.asr.2024.05.059

such scenarios, it becomes necessary to consider the assignment and service sequence of the client satellites, as well as optimize the trajectory of the service spacecraft to each client satellite to maximize the OOR mission's profit (Zhang et al., 2022). This gives rise to the problem of OOS mission planning.

The mission planning of multiple OOS spacecraft and client satellites has been well studied recently. Zhang et al. (2014) studied the multispacecraft refueling mission planning with the J_2 perturbation and time window constraints by a hybrid-encoding multi-objective genetic algorithm. Du et al. (2015) also focused on the multi-spacecraft refueling mission and developed a model with a cooperative maneuver of service spacecraft and client satellites. The results indicated that the cooperative strategy could significantly save fuel costs. Cerf (2015) studied the mission planning problem of multiple low earth orbit space debris successive removal. Bang and Ahn (2019) developed a two-phase framework for multi-target active debris removal mission problems. Baranov et al. (2020) studied the debris removal mission planning problem under two cases: one is placing the thruster deorbiting kits in the debris and another is taking the debris to the disposal orbit by the service satellite. Wei et al. (2021) also studied the geostationary debris removal mission under a hybrid-propulsive service spacecraft, which can significantly reduce the fuel cost in maneuvering between two space debris. Han et al. (2023) studied the on-orbit refueling problem for satellites in sun-synchronous orbit; the fuel station's position and service spacecraft's refuel schedule are jointly optimized to reduce the total fuel cost. We can see that optimization of fuel consumption is a paramount consideration in the context of mission planning. Thus, in this paper, we also focus our attention on two on-orbit service tasks, namely on-orbit refueling and debris removal. These two tasks result in changes to the satellite's mass, a key factor that significantly influences the total fuel consumption during orbit transfer.

In the above research results, the mission planning problem has usually been formulated as a mixed-integer nonlinear programming (MINLP) model, which is hard to solve by commercial solvers like Cplex and Gurobi. Various metaheuristic algorithms and their variants such as genetic algorithm (GA) (Zhang et al., 2014; Jia et al., 2023; Du et al., 2015; Zhao et al., 2017), particle swarm optimization (PSO) (Zhou et al., 2015b; Chen and Yu, 2017; Daneshjou et al., 2017), ant colony optimization (ACO) (Li and Baoyin, 2019; Zhang et al., 2022; Shen et al., 2018; Chen et al., 2021), and simulated annealing algorithm (SA) (Han et al., 2019; Li and Xu, 2020) have been used to solve the problem due to their feasibility in large-scale and complex optimization problems.

In practical engineering, the consideration of uncertainty is of paramount importance. Similarly, in the domain of multi-satellite mission planning, the existing uncertainty is a crucial factor that requires due attention, yet it is often overlooked. The cloud coverage uncertainty is widely considered in the earth observation mission of agile satellites (Han et al., 2022a; Wang et al., 2018). Lots of optimization models are formulated, such as the stochastic integer programming model (Liao and Yang, 2007), the robust model (Tangpattanakul et al., 2012), etc. However, most existing research on the on-orbit mission has assumed that the state of targets is known and fixed, ignoring the uncertainties in the state of targets. Jonchay et al. (2020); Jonchay et al. (2021) considered four different random service needs of on-orbit service: repositioning, retirement, repair, and mechanism deployment. They developed a framework for modeling and optimization of on-orbit servicing operations under demand uncertainties. However, they still regarded the refueling, inspection, and station keeping as deterministic needs. Thus, it is necessary to consider other uncertainties of on-orbit missions.

The operational satellites must maintain their designated orbital slot to successfully carry out various tasks, such as the observation mission. However, the on-orbit satellites need to perform orbital maneuvers to fix the orbit error caused by orbit perturbation. This necessitates the utilization of these satellites' remaining fuel reserves. Thus, the final service fuel demand may deviate from the initial fuel demand, which is the fuel uncertainty considered in this paper. Additionally, there is also uncertainty surrounding the capture of the debris. The majority of space debris is tumbling due to its residual angular momentum (Shan et al., 2016), making it challenging to obtain comprehensive and detailed information about the specific debris. Besides, de-tumbling brings great trouble for capturing with a robotic arm. Thus, there is also a risk of failure in capturing debris. This paper focuses on space debris that is produced in the hypervelocity impact with spacecraft walls, high-intensity explosion, or low-intensity explosion, rather than dysfunctional satellites and rocket upper stages. For the GEO debris removal, removing large-size debris to the graveyard orbit is a common method (Yu et al., 2014). However, in the hybrid mission that includes both on-orbit refueling and debris removal, this strategy is no longer suitable. The transfer cost of service satellite with heavy fuel to the graveyard orbit will be high and even beyound the profit of the debris cleaning. Besides, we assume that the size of the debris we considered is not large and has a low mass, and there is no need to transport it to a graveyard orbit for disposal. Thus, this paper aims to address the uncertainty in hybrid mission planning problems associated with the demand for on-orbit service tasks, specifically on-orbit refueling and debris removal.

To the best of the authors' knowledge, there is little research on continuous OOS missions with uncertainties in refueling demand and debris capture probability. Motivated by the discussion, this paper models the mixed on-orbit refueling and debris removal mission planning problem using two distinct optimization techniques to manage

the uncertainty of the two-stage situation. A comparison of the differences between these two types of models under various simulation conditions is also provided.

The primary contributions of this study can be summarized as follows:

(1) The concept of hybrid uncertainty in OOS mission planning is being explored in this study. A novel stochastic expectation model has been developed to quantify this uncertainty, which can get the optimal expected benefits.

(2) A robust model considering hybrid uncertainty has been proposed. It can still achieve the best benefits under the worst situation, which has been rarely considered in the OOS mission planning field.

The rest of the paper is organized as follows: Section 2 gives the Problem Statement and the Multi-Pulse Maneuvering Orbit Transfer Strategy. Sections 3 and 4 present the Stochastic Expectation Model Considering Uncertainty and Robust Model Considering Box Uncertainty, respectively. Section 5 verifies the proposed algorithm through simulation and compares two proposed models. The conclusion of this work is drawn in Section 6.

2. Problem statement and orbit maneuver model

2.1. Problem statement

To optimize cost efficiency, we have taken into account the possibility of a single service satellite being able to perform multiple on-orbit fueling and space debris removal tasks consecutively efficiently, as shown in Fig. 1. The uncertainties associated with on-orbit service have been carefully considered during the task planning phase. For the space debris removal, the probability $P(Sc)$ of the event successfully capturing the target Sc is considered. The uncertainties of debris removal are binary-valued parameters. If the debris removal task succeeds, the service satellite's mass increases. Otherwise, it is constant. On the other hand, the primary uncertainty in the on-orbit refueling task lies in the fuel demand. Since transferring the service satellite's orbit is time-consuming, the client satellite typically requires fuel consumption to correct its orbit during this period. It is assumed that the uncertain fuel demand ω_i conforms to a normal distribution (Gaussian distribution), i.e., $\omega_i \sim N(\mu_i, \sigma_i^2)$.

During the planning phase, the challenges of on-orbit refueling and debris removal are considered as the final rendezvous problem. For convenience, space debris and client satellites are all called targets. Assuming that if the service satellite is positioned in the orbit of the target, the rendezvous can be successfully accomplished.

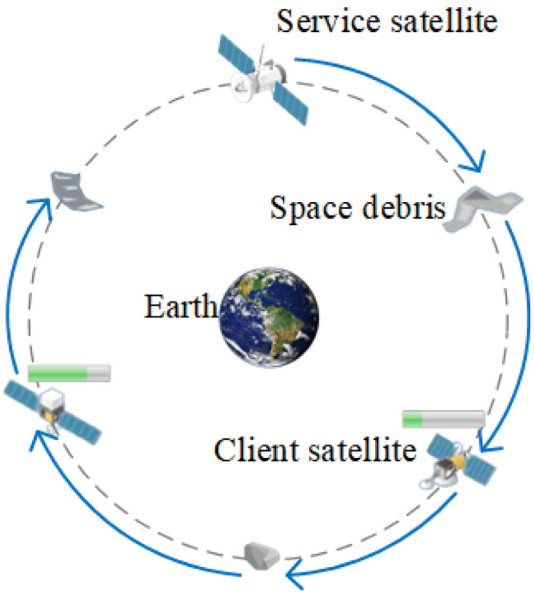

Fig. 1. The illustration of the on-orbit refueling and debris removal hybrid mission.

2.2. Multi-pulse maneuvering orbit transfer

The service satellite's total mass is relatively high due to the need to carry a significant amount of fuel or drag large-mass space debris. To minimize fuel consumption, the transfer orbits strategy requires lower pulse maneuvers. Considering that the time constraint for orbit transfer is usually not urgent in space, reducing fuel consumption is the highest priority. We assume that the geosynchronous satellite orbits are circular orbits with different orbital inclinations and radii, which means the eccentricity is zero. The orbit transfer contains two parts: adjusting orbit plane and Hohmann orbit transfer to adjust the radius.

2.2.1. Ascent for satellite orbit

First, consider the case of ascent for satellite orbit, in which the service satellite transfers from the high orbit to the low orbit. The speed of an orbit decreases as its altitude increases. Therefore, as shown in Fig. 2, the steps are:

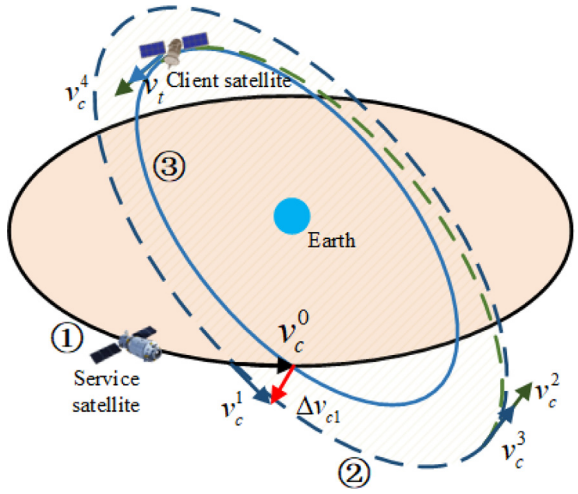

Fig. 2. The illustration of ascent for satellite orbit.

- the adjustment of the orbit plane at the intersection point of orbit ① and ②.
- the Hohmann orbit transfer to adjust the orbit height.

In total, three pulse maneuvers are performed.

While changing the orbital plane, as shown in Fig. 3, we take the projection of original velocity $\boldsymbol{v}_c^0$ at the intersection of two orbits from the initial orbit to the target orbital plane as the velocity $\boldsymbol{v}_c^1$ after maneuvering to minimize the pulse maneuver. The angle of two orbits can be calculated as

$$\cos\alpha = \sin I_c \sin I_t \cos(\Omega_c - \Omega_t) + \cos I_s \cos I_t \tag{1}$$

where $I_c, I_t, \Omega_c, \Omega_t$ is the orbital inclination and right ascension of ascending node of the target and service satellite respectively. Besides, the two points of intersection of two orbits can be obtained by

$$\begin{cases} \boldsymbol{r}_1 & = a_c \frac{\boldsymbol{h}_c \times \boldsymbol{h}_t}{\|\boldsymbol{h}_c \times \boldsymbol{h}_t\|} \\ \boldsymbol{r}_2 & = -\boldsymbol{r}_1 \end{cases} \tag{2}$$

where a_c is the orbital radius of the service satellite, $\boldsymbol{h}_c$ and $\boldsymbol{h}_t$ is the angular momentum of the orbits of the service satellite and target respectively. The angular momentum of the orbit can be calculated by

$$\boldsymbol{h} = \sqrt{\alpha\mu} \begin{bmatrix} \cos\Omega & -\sin\Omega & 0 \\ \sin\Omega & \cos\Omega & 0 \\ 0 & 0 & 1 \end{bmatrix} \begin{bmatrix} 1 & 0 & 0 \\ 0 & \cos i & \sin i \\ 0 & \sin i & \cos i \end{bmatrix} \begin{bmatrix} 0 \\ 0 \\ 1 \end{bmatrix} \tag{3}$$

where μ is standard gravity parameters. Therefore, according to $\boldsymbol{h} = \boldsymbol{r} \times \boldsymbol{v}$, we can obtain the velocity $\boldsymbol{v}_c^0$ at the intersection of two orbits. So the pulse maneuver of plane change is

$$\Delta\boldsymbol{v}_{c1} = \boldsymbol{v}_c^0 - \boldsymbol{v}_c^1 \tag{4}$$

$$\Delta v_{c1} = \|\Delta\boldsymbol{v}_{c1}\| = \left\|\Delta\boldsymbol{v}_c^0\right\| \sin\alpha \tag{5}$$

After completing the maneuver of plane change, the orbit of the service satellite becomes an elliptical orbit coplanar with the target orbit. The velocity $\boldsymbol{v}_t$ and position $\boldsymbol{r}_t$ of the target at some point are selected as two bases of the target orbital plane. According to the projection principle, the velocity $\boldsymbol{v}_c^1$ of service satellite after changing plane can be calculated as

$$\boldsymbol{v}_1^c = A(A^{\mathrm{T}}A)^{-1}A^{\mathrm{T}}\boldsymbol{v}_c^0 \tag{6}$$

where $A = [\boldsymbol{r}_t, \boldsymbol{v}_t]$. Then, the new orbit can be determined by the velocity $\boldsymbol{v}_1^c$ and the position $\boldsymbol{r}_c^0$ at the intersection. The six orbital elements $(a_n, e_n, i_n, \Omega_i, \omega_i, \theta_i)$ of the new orbit can also be obtained.

Next, the Hohmann orbit transfer strategy is used to transfer to the target orbit, which is the optimal orbit in the case of co-planer transfer. Considering that the initial orbit is a circle orbit and the velocity reduced after planner change, the new orbit is elliptical and the intersection is the apogee of the new orbit. As shown in Fig. 3, for an elliptical orbit transferred to the inner circular orbit, the optimal transfer orbit should start at the apogee of the outer elliptical orbit. So the eccentricity of the transferred Hohmann orbit is

$$e_h = \frac{a_c - a_t}{a_t + a_c} \tag{7}$$

where a_t is the semi-major axis of the target, that is the radius of the target. At first, the angular momentum of the Hohmann orbit can be calculated by

$$h_h = \sqrt{r_c\mu(1 - e_h)} \tag{8}$$

The velocity v_c^3 of start point and the velocity v_c^4 of end point in transfer orbit is

$$v_c^3 = \frac{h_h}{r_c} \tag{9}$$

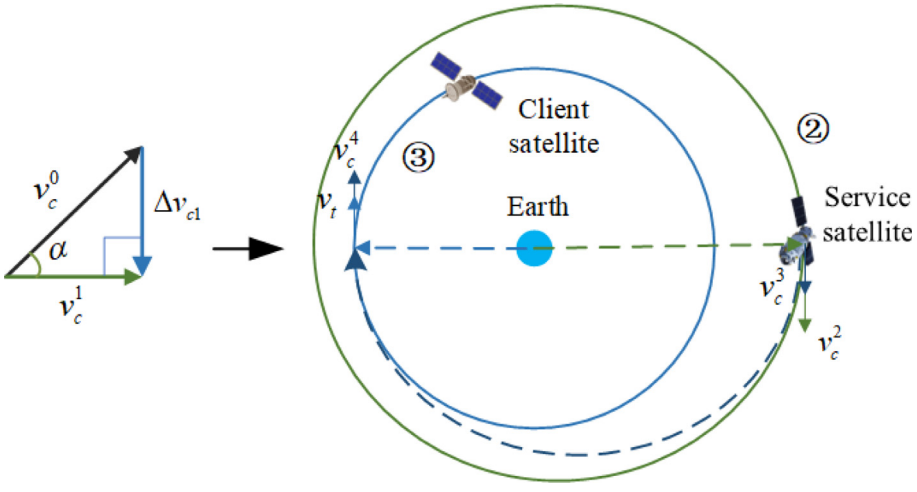

Fig. 3. The steps of ascent for satellite orbit.

$$v_c^4 = \frac{h_h}{r_t} \tag{10}$$

The velocity vectors at the start point and the endpoint of the Homann orbit are tangent to the orbit of the service satellite and the orbit of the target respectively, so the velocity before the maneuvering pulse is in the same direction as the velocity after the maneuvering, thus the two required impulse maneuvers for the Homann orbit can be obtained by:

$$\Delta v_{c2} = \left| v_c^2 - v_c^3 \right| \tag{11}$$

$$\Delta v_{c3} = \left| v_t - v_c^4 \right| \tag{12}$$

Therefore, in the case of the transfer from high orbit to low orbit, the total pulse maneuver is

$$\Delta v = \Delta v_{c1} + \Delta v_{c2} + \Delta v_{c3} \tag{13}$$

2.2.2. Descent for satellite orbit

As shown in Fig. 4, the target is on a higher orbit and has lower velocity in this situation. Hence, the strategy of descent for service satellite orbit is:

- The Hohmann orbit involved an initial maneuver to attain the identical orbital altitude as the intended orbit
- A transfer of the orbit plane to align with the target plane.

As shown in Fig. 5, at first, the Hohmann orbit is used to transfer from a circular orbit to another circular orbit. Similarly, Hohmann orbit can be calculated, of which the apogee is on the target orbit, and the perigee is on the service satellite orbit. The value of its angular momentum is:

$$h_h = \sqrt{r_c \mu (1 + e_h)} \tag{14}$$

Thus, the total pulse maneuver of the Hohmann transfer is

$$\Delta v_h = \frac{h_h}{r_c} + \frac{h_h}{r_t} \tag{15}$$

After the Hohmann orbit transfer, the height of the new circular orbit is the same as the target one. So for the orbit planer adjustment, the velocity keeps the same value with different directions, as shown in Fig. 5. The corresponding maneuvering pulse is

$$\Delta v_{c1} = 2 v_t \sin\left(\frac{\alpha}{2}\right) \tag{16}$$

where α is also the angle of two orbits. Therefore, the total impulse maneuver of the transfer orbit is

$$\Delta v = \Delta v_h + \Delta v_{c1} \tag{17}$$

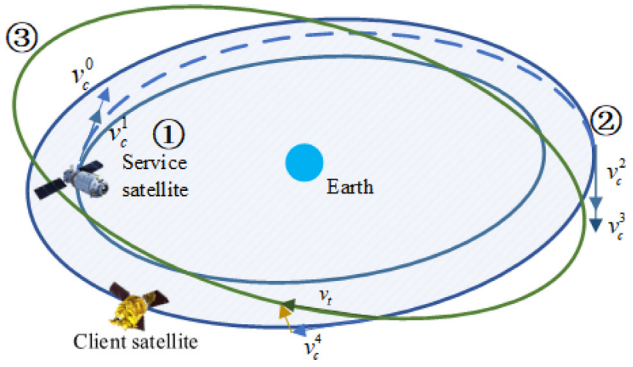

Fig. 4. Orbit transfer from low orbit to high orbit.

2.3. Directed graph of on-orbit servicing tasks

The above-mentioned orbit transfer strategy determines the construction of the directed graph of the on-orbit service mission. The service satellite needs to perform three pulse maneuvers to perform on-orbit service for each target. We consider not only the constraint pulse maneuver value but also the constraint of the change in the mass of service satellites resulting from fuel changes. Define the three maneuver pulse as $\Delta v_1, \Delta v_2, \Delta v_3$ and the corresponding fuel consumption as $\Delta m_1, \Delta m_2, \Delta m_3$. The total mass of the service satellite before orbit changing is M. Then, the mass change Δm in the total fuel required for each transfer to the orbit of the target can be represented by

$$\begin{aligned}\Delta m &= \Delta m_1 + \Delta m_2 + \Delta m_3 \\ &= \left(1 - e^{\frac{-\Delta v_1}{I_{sp} g_0}}\right) M + \left(1 - e^{\frac{-\Delta v_2}{I_{sp} g_0}}\right)\left(M - \Delta m_1\right) \\ &\quad + \left(1 - e^{\frac{-\Delta v_3}{I_{sp} g_0}}\right)\left(M - \Delta m_1 - \Delta m_2\right) \\ &= \left(1 - e^{\frac{-\Delta v}{I_{sp} g_0}}\right) M\end{aligned} \tag{18}$$

where M is the total mass of the service satellite before maneuvering, g_0 is the gravitational acceleration at sea level. I_{sp} is the specific thrust of fuel, representing the propulsion system's ability. The specific thrust of commonly used fuel liquid oxygen and liquid hydrogen is 455 s.

Considering the limited pulse maneuverability of the service satellite, the maximum value of a single pulse is around 400 m/s. It is postulated that in the event that any of the three pulse maneuvers involved in the orbit transfer procedure surpasses the capacity of a solitary maneuver, it is deemed unfeasible to establish a connection. Therefore, we can give the directed connection graph between the service satellite and each target. As shown in Fig. 6, we set a virtual endpoint and require the service satellite to reach the virtual endpoint after all targets have been served. According to the Eq. (18), the transfer cost is related to the mass of the service satellite. Thus, the first orbit transfer from the initial orbit of the service satellite to the target has a fixed cost, while the transfer cost between the targets (green solid line) changes depending on the service sequence. Consequently, certain targets are interconnected in a two-way manner, some are connected in a one-way fashion, and others are not connected at all. For conve-

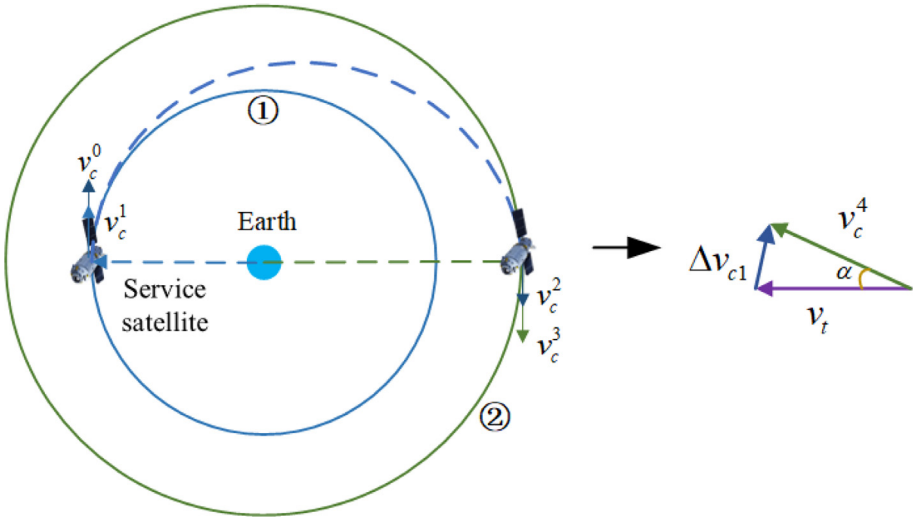

Fig. 5. The steps of orbit descent.

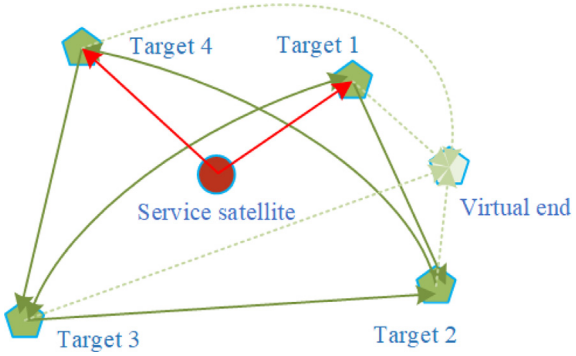

Fig. 6. Orbit transfer connected directed graph of service satellite and target.

nience, every target is linked to a virtual endpoint with no transfer cost involved.

3. Stochastic expectation model considering uncertainty

The uncertainty makes the service's benefits and costs difficult to predict. Our proposed stochastic expectation model aims to determine the service sequence that yields the highest expected benefits. A stochastic expected value programming model based on flow variables is established considering the above two kinds of uncertainties. Define binary decision variables

$$x_{ij}^k = \begin{cases} 1, & \text{the service satellite transfers from target i to j in } k^{\text{th}} \text{ transfer} \\ 0, & \text{otherwise} \end{cases} \tag{19}$$

where $i \in T \cup \{s\}, j \in T \cup \{e\}, k \in O$. T is the set of targets with n elements. s is the starting point of the service satellite. e is the virtual endpoint. k represents the servicing sequence. $O = \{1, 2, \cdots, n+1\}$ is the set of transfer paths of the service satellite, as there are totally $(n+2)$ points and $(n+1)$ paths to connect them. The mass change of the service satellite is used in the objective function to unify the gains and costs of on-orbit service. The stochastic expectation model is formulated as a constrained nonlinear optimization problem.

First, the objective function (20) represents the difference between the overall expected benefit of the on-orbit servicing mission and the weighted expected transfer cost of completing the mission, $|\omega_i|$ represents the expected benefit of target i. The servicing benefit is the mass of the fuel required by the client satellite. Assuming that the fuel value required by each client satellite is between $[m_{\min}^i, m_{\max}^i]$ and meets a certain distribution probability, which can defined as ω_i; Since dragging debris will increase the weight of the service satellite, in order to distinguish it from fueling task, the benefit of the cleaning task is ω_i is negative. So, for the space debris with mass m_i and the probability of completing the cleaning task $p_i \in [0, 1]$, the corresponding expected benefit is $-\omega_i = p_i m_i$. The cost of the task is the mass change caused by the pulse maneuver of each transfer from the service satellite to the target, that is, the mass of fuel consumed by the pulse maneuver Δm_{ij}^k, which can be calculated by (21). At the same time, the weight parameters $\lambda_w$and λ_m can be adjusted to change the proportion between the expected benefit and the cost. Therefore, this model aims to maximize the expected benefit minus the expected cost.

$$\max_{x_{ij}^k} \sum_{i \in T \cup \{s\}} \sum_{\substack{j \in T \cup \{e\} \\ j \neq i}} \sum_{k \in O} (\lambda_w \mid \omega_i \mid x_{ij}^k - \lambda_m \Delta m_{ij}^k x_{ij}^k) \tag{20}$$

$$\Delta m_{ij}^k = \left(1 - e^{\frac{-\Delta v_{ij}}{I_{sp} g_0}}\right) \times \left(M - \sum_{\hat{i} \in T \cup \{s\}} \sum \sum_{k < k} (\Delta m_{\hat{i}\hat{j}}^{\hat{k}} + \omega_{\hat{i}}) x_{\hat{i}\hat{j}}^{\hat{k}}\right), \forall x_{ij}^k = 1 \tag{21}$$

where M is the mass of the service satellite before serving. The mass change after the completion of an on-orbit service mission comes from the fuel reduction of the refueling mission or the increase of the debris mass and the fuel con-

sumption during the transfer process. The following gives the constraints of this problem:

$$s.t. \quad \sum_{j\in T} x_{sj}^{1} = 1 \tag{22a}$$

$$\sum_{i\in T\cup\{s\}} \sum_{\substack{j\in T\cup\{e\}\\ j\neq i}} x_{ij}^{k} = 1, \forall k \in O \tag{22b}$$

$$\sum_{\substack{j\in T\cup\{e\}\\ j\neq i}} \sum_{k\in O} x_{ij}^{k} = 1, \forall i \in T \tag{22c}$$

$$\sum_{i\in T} x_{ie}^{n+1} = 1 \tag{22d}$$

$$\sum_{k\in O} \sum_{\substack{j\in T\cup\{e\}\\ j\neq i}} x_{ij}^{k} = \sum_{k\in O-\{1\}} \sum_{\substack{j\in T\cup\{e\}\\ j\neq i}} x_{ji}^{k-1}, \forall i \in T \tag{22e}$$

$$\sum_{k\in O} x_{ij}^{k} = 0, \forall L_{ij} = 0 \tag{22f}$$

$$\sum_{i\in T\cup\{s\}} \sum \sum_{k\in O} m_{ij}^{k} x_{ij}^{k} + \sum \sum \sum_{k\in O} \omega_i x_{ij}^{k} < M_f \tag{22g}$$

$$x_{ij}^{k} \in \{0, 1\} \tag{22h}$$

The Eq. (22a) represents the start point constraint: the first path of the service satellite is from the start point to and only to a certain target. The Eq. (22b) is the path unique constraint: each path of the service satellite is unique; The Eq. (22c) gives the full ergodic constraints: each target has been served; The virtual endpoint constraint shows as (22d): the path of the service satellite ends at the virtual node. The flow balance constraint, as stated in (22e), ensures that the quantity of incoming paths for every target point remains equivalent to the quantity of outgoing paths. The Eq. (22f) makes sure the directed connected graph constraint: L_{ij} is the element in row i and column j of the adjacency matrix. If $L_{ij} = 1$, from i to j are connectable, otherwise, it is not connectable. The inequality (22g) is the constraint on the total fuel carried by the service satellite: the total amount of fuel refueled by targets and the total fuel required during the transfer process must not exceed the total fuel carried by the service satellite M_f. The last one (22h) gives the search space of the decision variables.

The integer nonlinear programming problem represented in the aforementioned random expectation model is typically addressed through the utilization of the branch and bound method. Originally devised to tackle discrete programming problems, the branch and bound method has emerged as the predominant approach for resolving NP-hard problems,including the renowned traveling salesman problem (Jünger et al., 1995).In the context of this problem, the orbit transfer strategy disregards the time constraint, rendering it akin to the traveling salesman problem. Consequently, the branch and bound method can be employed to resolve it effectively.

The branch and bound method first divides the feasible solution space into smaller solution subsets and then mainly relies on two subroutines, which need to calculate the upper bound and lower bound of the optimal value of a given area, respectively, called an upper solver and a lower solver. The upper bound solver can find the upper bound by selecting any point in the region or by local optimization methods, the lower bound can be found from convex relaxation, dual, Lipschitz or other bounds. In conclusion, the basic idea of this algorithm is as follows: At first, divide the feasible set into convex sets, find the lower limit/upper limit for each convex set, and then form the global upper and lower bounds, if the two bounds are close enough, the algorithm will stop; otherwise, it will continue to refine repeatedly.

This model is a special $0-1$ integer programming model, the decision variable x_{ij}^{k} can only be 0 or 1. At this time, a particular branch and bound method, that is, an implicit enumeration method, is required. The specific steps of the algorithm are as follows:

(1) Preprocessing: Since this model solves the maximum value problem, the objective function needs to add a negative sign and be converted into a standard mode for solving the minimum value.

(2) First enumerate without considering constraints, initially starting from $x_{ij}^{k} = 0$.

(3) Check whether it satisfies the constraint conditions; if there is any dissatisfaction, continue enumeration (execute (2)); if all constraints are satisfied, it is a feasible solution, and then calculate its objective function (execute (4)).

(4) Calculate the objective function, if it is greater than the function value of the existing feasible solution, then prune; if it is less than the existing feasible solution, then update the feasible solution and the objective function value, and continue enumeration on this branch (execute (2)).

4. Robust model considering box uncertainty

In the field of aerospace engineering, it is common practice to employ conservative approaches. Hence, we also developed a robust model that can get the service sequence with the best benefits in the worst situation. The considered uncertainty is the benefit obtained from the client satellites or the debris which will also affect the transfer cost of the service satellite. The basic idea of robustness is to consider the poorest situation, which means the failure of the debris capture and the lowest benefit from the on-orbit refueling. This section uses this idea to model and optimize this uncertainty problem. Box uncertainty is a relatively simple and common representation of uncertainty, which gives the boundary of the uncertainty and does not complicate the model.

The objective function (23) is still defined as the difference between the benefit of the on-orbit service and the

orbit transfer cost. And the decision variables are still defined as $x_{ij}^k \in \{0,1\}$. Similarly, the proportion between the expected benefit and the cost is adjusted by changing the weight parameters λ_w and λ_m. Different from (20), the mass change of the service satellite is defined as an uncertainty parameter $|W_i|$ instead of the expected benefit $\|\omega_i\|$. The mathematical model of this optimization problem is shown as follows:

$$\max_{x_{ij}^k} \quad \sum_{i\in T\cup\{s\}}\sum_{\substack{j\in T\cup\{e\}\\ j\neq i}}\sum_{k\in O}(\lambda_w \mid W_i \mid x_{ij}^k - \lambda_m \Delta m_{ij}^k x_{ij}^k) \tag{23}$$

$$\begin{aligned}&\Delta m_{ij}^k = (1 - e^{\frac{-\Delta v_{ij}}{I_{sp}g_0}})\\ &\times(M - \sum_{\hat{i}\in T\cup\{s\}}\sum\sum_{\hat{k}<k}(\Delta m_{\hat{i}\hat{j}}^{\hat{k}} + W_i)x_{\hat{i}\hat{j}}^{\hat{k}}), \forall x_{ij}^k = 1\end{aligned} \tag{24}$$

$$\text{s.t.} \quad WL_i \leqslant W_i \leqslant WH_i, \forall i \in T \tag{25a}$$

$$\sum_{j\in T} x_{sj}^1 = 1 \tag{25b}$$

$$\sum_{i\in T\cup\{s\}}\sum_{\substack{j\in T\cup\{e\}\\ j\neq i}} x_{ij}^k = 1, \forall k \in O \tag{25c}$$

$$\sum_{\substack{j\in T\cup\{e\}\\ j\neq i}}\sum_{k\in O} x_{ij}^k = 1, \forall i \in T \tag{25d}$$

$$\sum_{i\in T} x_{ie}^{n+1} = 1 \tag{25e}$$

$$\sum_{k\in O}\sum_{\substack{j\in T\cup\{e\}\\ j\neq i}} x_{ij}^k = \sum_{k\in O-\{1\}}\sum_{\substack{j\in T\cup\{e\}\\ j\neq i}} x_{ji}^{k-1}, \forall i \in T \tag{25f}$$

$$\sum_{k\in O} x_{ij}^k = 0, \forall L_{ij} = 0 \tag{25g}$$

$$\sum_{i\in T\cup\{s\}}\sum\sum_{k\in O}\Delta m_{ij}^k x_{ij}^k + \sum\sum\sum_{k\in O} W_i x_{ij}^k < M_f \tag{25h}$$

$$x_{ij}^k \in \{0,1\} \tag{25i}$$

Constraints related to directed graphs: Constraints (25a)–(25g) are consistent with (22a)–(22f) in the expectation model. They are related constraints to ensure that the service satellite reaches the virtual endpoint after servicing targets from the start point. As for the box uncertainty constraints (25a), the uncertain benefit changes continuously within an interval of which boundary is the predicted min and max required demand of the on-orbit refueling, that is, WL_i and WH_i. For the debris removal task, whether it can be removed is a binary problem, which is generally believed that the corresponding benefit can only be zero or the mass of the debris m_i^s, that is, $W_i = 0$ or $W_i = -m_i^s$. However, since the impact of the mass change of debris on the objective function is monotonous, robust optimization usually operates on the maximum or minimum value of uncertain parameters. To maintain the unified representation with the uncertainty of the on-orbit refueling task, the boundary of the debris removal task is $WL_i = -m_i^s, WH_i = 0$. The total fuel constraint (25h) carried by the service satellite is also a little different from the stochastic expectation model. The expected value in (21) and (22g) is replaced by W_i.

Compared with the stochastic expectation model, this robust model is more complicated. W_i is an uncertain parameter multiplied by decision variable x_{ij}^k, which makes the objective function more complex. The current model exhibits neither linearity nor quadratic characteristics, thereby deviating from the conventional operations research model. Unfortunately, there is no advanced solver available that can effectively address this type of problem.

Therefore, this paper disassembles this model into two parts. First, each target's transfer cost and benefit are not considered, and only the graph's connectivity is considered. By enumerating, all feasible solutions that satisfy the constraints except (25a) and (25h) are obtained; Then, the objective function optimization model under box uncertainty with the given service sequence can be solved; Finally, the optimal service sequence with the maximum objective function of the robust model can be given.

The recursive method is used to enumerate, as shown in Fig. 6, all solutions require starting from the service satellite and traversing all targets. The Algorithm 1 is the pseudo-code of this algorithm, which describes the search process for feasible solutions based on deep search, considering the connectivity constraints of the graph.

Algorithm 1. Depth-first based recursive traversal algorithm

Input: set of targets T, staring point s, adjacency matrix L
Output: set of all flexible paths S
1: $R(1) \leftarrow s$ // Initialize the first point of each feasible sequence as the starting point s
2: $R(j) \leftarrow \varnothing, (j \leftarrow 2,3,\cdots n+1)$ // The remaining positions of the initialized feasible sequence are all empty
3: $F(i) \leftarrow 0 (i \in T)$// Initialize the flag bit of each target to 0
4: $u = 2$
5: **call recursion** $< u, n, r, F >$
6: **program recursion** $< u, n, r, F >$
7: **if** $u > n+1$ **then**
8: $S \leftarrow \{S, R\}$// Output an iterated sequence to the set S
9: **end if**
10: **for** $i \leftarrow 1,2,\cdots,n$ **do**
11: **if** $F(i) = 0 \bigwedge L_{R_{u-1}i} = 1$ **then**
12: $r(u) \leftarrow i$ // If the target i has not been served and can be connected from the previous point to i, it is set as the next served target

(continued on next page)

13: $F(i) \leftarrow 1$
14: **call recursion** $< u+1, n, r, F >$
15: $F(i) \leftarrow 0$
16: **end if**
17: **end for**
18: **end program**

After obtaining all feasible sequences, solving each feasible sequence's optimal objective function under uncertainty needs to be solved. Robust optimization means the objective function obtains the optimal value when the uncertain parameters are the worst. Therefore, this subproblem needs to obtain the optimal objective function value under the worst case of different feasible sequences, that is, to maximize the lower bound of the target objective function defined as t. The new decision variable of this suboptimization problem is $t \in \mathbb{R}$. The robust subproblem is modeled as follows:

$$\min \quad t \tag{26}$$

$$\text{s.t.} \quad Z = \sum_{i \in T \cup \{s\}} \sum_{\substack{j \in T \cup \{e\} \\ j \neq i}} \sum_{k \in O} (\lambda_w \mid W_i \mid x_{ij}^k - \lambda_m \Delta m_{ij} x_{ij}^k) \geqslant -t \tag{27a}$$

$$x_{ij}^k \in r, \forall i \in T \cup \{s\}, j \in T \cup \{e\}, j \neq i, k \in O \tag{27b}$$

$$WL_i \leqslant W_i \leqslant WH_i, \forall i \in T \tag{27c}$$

$$\sum_{i \in T \cup \{s\}} \sum \sum_{k \in O} \Delta m_{ij}^k x_{ij}^k + \sum \sum \sum_{k \in O} W_i x_{ij}^k < M_f \tag{27d}$$

where t is the lower bound of the target objective function, since the standard robust problem is to solve the minimum problem, while the model (23) is to obtain the maximum, adding a minus sign is to prepossessed, that is, the constraint (27a). r represents a feasible solution obtained by traversal. Constraint (27b) makes x_{ij}^k known and no longer a decision variable, which greatly simplifies the complexity of the model. The constraint (27c) represents the box-like uncertainty of the uncertainty term W_i; likewise, the constraint (27d) represents limits on the overall fuel the serving satellite can carry.

From this, the lower bound of the target revenue corresponding to each feasible solution can be calculated, and the feasible solution with the largest lower bound is selected as the service sequence under uncertainty, which ensures that the target total benefit of this task is optimal even in the worst case.

5. Simulations

In this section, the simulation analysis of the one-to-many GEO satellite on-orbit service scenario is carried out to compare the effects of different models. Assume that the dry mass of the service satellite is 1000 kg, and the total amount of fuel it carries is 1500 kg, which can be used both for its own pulse maneuver and on-orbit refueling. For the two models, we use the mature solver YALMIP. The bmibnb solver is selected for solving integer programming problems, where fmincon is used as the upper bound solver, and the lower bound solver and LP solver both select GUROBI.

In the simulation scenario, five GEO circular orbits are selected as the targets, the detailed parameters are given in Table 1. The start time of the scenario is 2023–01-25 04:00:00. The orbital elements of the initial orbit of the service satellite are $(42162.261955\ \text{km}, 0, 55^\circ, 166^\circ, 0, 137^\circ)$. According to the orbit parameters, the adjacency matrix corresponding to this simulation scenario can be obtained as

$$L = \begin{bmatrix} 0 & 1 & 1 & 0 & 1 & 1 \\ 0 & 0 & 1 & 1 & 1 & 1 \\ 0 & 1 & 0 & 1 & 1 & 1 \\ 0 & 1 & 1 & 0 & 1 & 0 \\ 0 & 1 & 1 & 1 & 0 & 1 \\ 0 & 1 & 1 & 0 & 1 & 0 \end{bmatrix} \tag{28}$$

To better compare the different results of the two models based on the different uncertainties, we give the different simulations with different uncertainties.

Case 1: On-orbit Refueling Uncertainty.

We assume that the amount of on-orbit refueling required by the client satellites is a value within a certain range. According to the rule of 3σ, the fluctuation ranges of the required fuel are given as $[200, 300]$, $[170, 240]$, $[100, 300]$, $[150, 650]$, $[50, 60]$, the probability that the actual distribution in which is 99.73%. The corresponding expected values are 250 kg, 205 kg, 200 kg, 400 kg, 55 kg, respectively.

The stochastic expectation model and the robust model are both tested. Besides, the two kinds of weights are given. The results are shown in Table 2. The service sequences calculated by the two models are different. The stochastic expectation model gives the expected optimal benefits and the robust model gives the optimal lower bound. To ascertain the true impact, a series of 1000 random tests with the refueling demand consistent with normal distribution were carried out to simulate the benefit in real situations. The average value is pretty near to the result of the expectation model. Additionally, the minimum values closely approximate the outcome of the robust model, but both are bigger than it. It is due to the conservatism of the 3σ bound. Thus, the robust model of the on-orbit refueling uncertainty is conservative to some degree.

Case 2: Debris Remove Uncertainty.

In this simulation, we assume that there are five pieces of debris on the above-mentioned orbits. The masses of this

Table 1
Parameters of target orbits.

Number	Semimajor axis/km	Inclination/ °	RAAN/ °	Argument of Perigee/ °
1	42159.52485	55.159	169.36	189.776
2	42159.80077	54.217	173.801	180.929
3	42162.26196	54.485	176.311	226.918
4	42172.39465	55.11	173.37	224.043
5	42161.43459	58.536	168.957	157.879

Table 2
Comparison of optimization results of various models under uncertain on-orbit refueling.

Weights	Model	Optimization result	Optimal vaule	Average benefit of 1000 tests	Minimum benefit of 1000 tests
$\lambda_w = 0.05, \lambda_m = 1$	Stochastic expectation model	$s \to 1 \to 4 \to 3 \to 2 \to 5$	−283.6749	**−283.6648**	−337.6614
	Robust model	$s \to 1 \to 5 \to 4 \to 2 \to 3$	−375.8045	−288.0269	**−312.0496**
$\lambda_w = 1, \lambda_m = 1$	Stochastic expectation model	$s \to 1 \to 4 \to 3 \to 2 \to 5$	770.8251	**776.9102**	462.9982
	Robust model	$s \to 1 \to 5 \to 4 \to 2 \to 3$	293.0846	768.3955	**492.8975**

debris are 133 kg, 350 kg, 250 kg, 320 kg, 450 kg, and the probabilities of successful capture are $75\%, 90\%, 90\%, 85\%, 65\%$, respectively. The results of the two models are shown in Table 3. Similarly, the 1000 tests of two different model results are given. The sequence given by the expectation model has better average benefits, while the sequence given by the robust model has better minimum benefits. The capture task's reward is a binary variable, either zero or the mass of the debris, thus the lower bound of the benefits appears in the tests.

When fuel consumption of service satellites accounts for a higher share of benefits ($\lambda_w = 0.05, \lambda_m = 1$), the service sequences obtained by the two models are different. The order of No. 1 and No. 5 is opposite. It is due to the debris on orbit No. 5 with a large mass and a relatively low success capture probability. It is more robust to serve No. 5 after No. 1. However, the last three sequences are the same, indicating that not all uncertainties possess significant magnitude to impact the sequence.

Case 3: Hybrid Uncertainty.

For the hybrid tasks, we assume that the three client satellites waiting for refueling are on the first three orbits, of which the demands follow $N(120, (20/3)^2)$, $N(205, (35/3)^2), N(200, (100/3)^2)$, respectively. The other two orbits need to finish space debris removal tasks. The masses of the two debris are 350 kg and 310 kg, with corresponding success capture probabilities of 95% and 45%. The results are shown in Table 4, the average benefits of the service sequences provided by the stochastic expectation model are relatively higher, whereas the robust model yields greater minimum benefits. When faced with two models that have similar average benefits, opting for the robust one with significantly greater minimum benefits is a more feasible choice.

Table 3
Comparison of optimization results of various models under uncertainty of debris removal.

Weights	Model	Optimization Results	Optimal value	Average benefit of 1000 tests	Minimum benefit of 1000 tests
$\lambda_w = 0.05, \lambda_m = 1$	Stochastic expectation model	$s \to \mathbf{5} \to \mathbf{1} \to 4 \to 2 \to 3$	−394.8568	**−394.9883**	−431.6455
	Robust Model	$s \to \mathbf{1} \to \mathbf{5} \to 4 \to 2 \to 3$	−428.2009	−398.3228	**−428.2009**
$\lambda_w = 1, \lambda_m = 1$	Stochastic expectation model	$s \to 5 \to 1 \to 4 \to 2 \to 3$	620.9307	**624.1627**	−399.7054
	Robust Model	$s \to 5 \to 1 \to 4 \to 2 \to 3$	−399.7054	622.8174	**−399.7054**

Table 4
Comparison of optimization results of various models under hybrid uncertainty.

Weights	Model	Optimization Results	Optimal value	Average benefit of 1000 tests	Minimum benefit of 1000 tests
$\lambda_w = 0.05, \lambda_m = 1$	Stochastic expectation model	$s \to 1 \to 2 \to 3 \to 4 \to 5$	−337.9801	**−337.8413**	−366.1311
	Robust Model	$s \to 1 \to 5 \to 4 \to 2 \to 3$	−369.0360	−344.1677	**−361.9674**
$\lambda_w = 1, \lambda_m = 1$	Stochastic expectation model	$s \to 1 \to 2 \to 3 \to 4 \to 5$	799.1699	**797.4520**	213.6896
	Robust Model	$s \to 1 \to 5 \to 4 \to 2 \to 3$	67.9640	792.6311	**251.8473**

6. Conclusion

This study has proposed two optimization models to address the multi-satellite on-orbit service mission planning problem under uncertainty. The uncertainties encountered during on-orbit refueling and debris removal have been taken into account, as they influence the mass of the service satellite and consequently, the fuel consumption during the orbit transfer. A two-stage orbit transfer strategy (Hohmann orbit transfer and orbit plane adjustment) has been introduced to conserve fuel for maneuvering and to establish the directed graph between satellites or debris. The stochastic expectation model has been utilized to obtain the service sequence with the optimal average benefit, while the robust model has been employed to consider the worst-case scenario and provide the optimal minimum benefit. Simulations of GEO satellites show the different effects of the two proposed models.

This research novelty considers the uncertainty in the on-orbit service mission planning problem. However, there are instances where the level of uncertainty is not significant enough to impact the service sequence. Therefore, further research is required to accurately identify and quantify the influence of different levels of uncertainty.

Declaration of Competing Interest

The authors declare that they have no known competing financial interests or personal relationships that could have appeared to influence the work reported in this paper.

Acknowledgements

This work is supported by the National Natural Science Foundation of China (No. 62273118, No. 61973100, No. 12150008), Natural Science Foundation of Heilongjiang Province (LH2022F023), and Postdoctoral Fellowship Program of CPSF (GZB20230955).

References

Aglietti, G.S., Taylor, B., Fellowes, S., et al., 2020. The active space debris removal mission removedebris. part 2: In orbit operations. Acta Astronaut. 168, 310–322.

Bang, J., Ahn, J., 2019. Multitarget rendezvous for active debris removal using multiple spacecraft. J. Spacecr. Rock. 56 (4), 1237–1247.

Baranov, A., Grishko, D., Khukhrina, O., et al., 2020. Optimal transfer schemes between space debris objects in geostationary orbit. Acta Astronaut. 169, 23–31.

Cerf, M., 2015. Multiple space debris collecting mission: optimal mission planning. J. Optim. Theory Appl. 167 (1), 195–218.

Chen, S.-Y., Jiang, F.-H., Li, H.-Y., et al., 2021. Optimization for multitarget, multispacecraft impulsive rendezvous considering j2 perturbation. J. Guid., Control, Dynam. 44 (10), 1811–1822.

Chen, X.-Q., Yu, J., 2017. Optimal mission planning of GEO on-orbit refueling in mixed strategy. Acta Astronaut. 133, 63–72.

Daneshjou, K., Mohammadi-Dehabadi, A., Bakhtiari, M., 2017. Mission planning for on-orbit servicing through multiple servicing satellites: A new approach. Adv. Space Res. 60 (6), 1148–1162.

Du, B.-X., Zhao, Y., Dutta, A., et al., 2015. Optimal scheduling of multispacecraft refueling based on cooperative maneuver. Adv. Space Res. 55 (12), 2808–2819.

Forshaw, J.L., Aglietti, G.S., Fellowes, S., et al., 2020. The active space debris removal mission removedebris. part 1: From concept to launch. Acta Astronaut. 168, 293–309.

Han, C., Gu, Y., Wu, G., et al., 2022a. Simulated annealing-based heuristic for multiple agile satellites scheduling under cloud coverage uncertainty. IEEE Trans. Syst., Man, Cybernet.: Syst. 53 (5), 2863–2874.

Han, C., Zhang, S.-H., Wang, X.-W., 2019. On-orbit servicing of geosynchronous satellites based on low-thrust transfers considering perturbations. Acta Astronaut. 159, 658–675.

Han, P., Guo, Y., Li, C., et al., 2022b. Multiple geo satellites on-orbit repairing mission planning using large neighborhood search-adaptive genetic algorithm. Adv. Space Res. 70 (2), 286–302.

Han, P., Guo, Y., Wang, P., et al., 2023. Optimal orbit design and mission scheduling for sun-synchronous orbit on-orbit refueling system. IEEE Trans. Aerosp. Electron. Syst. 59 (5), 4968–4983.

He, H., Shi, P., Zhao, Y., 2023. Adaptive connected hierarchical optimization algorithm for minimum energy spacecraft attitude maneuver path planning. Astrodynamics 7 (2), 197–209.

Jia, G., Zhaojun, P., Zhonghua, D., 2023. Optimal planning for a multi-debris active removal mission with a partial debris capture strategy. Chin. J. Aeronaut.

Sarton du Jonchay, T., Chen, H., Gunasekara, O. et al. (2020). Rolling horizon optimization framework for the scheduling of on-orbit servicing operations under servicing demand uncertainties. In: ASCEND 2020 (p. 4131).

Sarton du Jonchay, T., Chen, H., Gunasekara, O., et al., 2021. Framework for modeling and optimization of on-orbit servicing operations under demand uncertainties. J. Spacecr. Rock. 58 (4), 1157–1173.

Jünger, M., Reinelt, G., Rinaldi, G., 1995. The traveling salesman problem. Handbooks Oper. Res. Manage. Sci. 7, 225–330.

Li, C.-Z., Xu, B., 2020. Optimal scheduling of multiple Sun-synchronous orbit satellites refueling. Adv. Space Res. 66 (2), 345–358.

Li, H.-Y., Baoyin, H., 2019. Optimization of multiple debris removal missions using an evolving elitist club algorithm. IEEE Trans. Aerosp. Electron. Syst. 56 (1), 773–784.

Liao, D.-Y., Yang, Y.-T., 2007. Imaging order scheduling of an earth observation satellite. IEEE Trans. Syst., Man, Cybernet., Part C (Appl. Rev.) 37 (5), 794–802.

Meng, B., Huang, J.-B., Li, Z., et al., 2019. The orbit deployment strategy of OOS system for refueling near-earth orbit satellites. Acta Astronaut. 159, 486–498.

Peng, C., Zhang, J., Yan, B., et al., 2021. Multisatellite flyby inspection trajectory optimization based on constraint repairing. Aerospace 8 (9), 274.

Redd, N.T., 2020. Bringing satellites back from the dead: Mission extension vehicles give defunct spacecraft a new lease on life-[news]. IEEE Spectr. 57 (8), 6–7.

Shan, M., Guo, J., Gill, E., 2016. Review and comparison of active space debris capturing and removal methods. Prog. Aerosp. Sci. 80, 18–32.

Shen, H.-X., Zhang, T.-J., Casalino, L., et al., 2018. Optimization of Active Debris Removal Missions with Multiple Targets. J. Spacecr. Rock. 55 (1), 181–189.

Sorenson, S.E., Pinkley, S.G.N., 2023. Multi-orbit routing and scheduling of refuellable on-orbit servicing space robots. Comput. Industr. Eng. 176, 108852.

Tangpattanakul, P., Jozefowiez, N., & Lopez, P. (2012). Multi-objective optimization for selecting and scheduling observations by agile earth observing satellites. In Parallel Problem Solving from Nature-PPSN XII: 12th International Conference, Taormina, Italy, September 1–5, 2012, Proceedings, Part II 12 (pp. 112–121). Springer.

Wang, J., Demeulemeester, E., Hu, X., et al., 2018. Exact and heuristic scheduling algorithms for multiple earth observation satellites under uncertainties of clouds. IEEE Syst. J. 13 (3), 3556–3567.

Wei, Z., Long, T., Shi, R., et al., 2021. Scheduling optimization of multiple hybrid-propulsive spacecraft for geostationary space debris removal missions. IEEE Trans. Aerosp. Electron. Syst. 58 (3), 2304–2326.

Yao, T.-Y., 2016. Refueling test system completed in-orbit verification. Aerospace China 3.

Yu, J., Chen, X.-Q., Chen, L.-H., et al., 2014. Optimal scheduling of GEO debris removing based on hybrid optimal control theory. Acta Astronaut. 93, 400–409.

Zhang, J., Parks, G.T., Luo, Y.-Z., et al., 2014. Multispacecraft refueling optimization considering the J2 perturbation and window constraints. J. Guid., Control, Dynam. 37 (1), 111–122.

Zhang, N., Chen, S., Zhang, Z., et al., 2022. Two-stage dynamic-assignment optimization method for multispacecraft debris removal. J. Guid., Control, Dynam. 45 (9), 1750–1759.

Zhao, Z., Zhang, J., Li, H.-Y., et al., 2017. LEO cooperative multi-spacecraft refueling mission optimization considering J2 perturbation and target's surplus propellant constraint. Adv. Space Res. 59 (1), 252–262.

Zhou, Y., Yan, Y., Huang, X., et al., 2015a. Mission planning optimization for multiple geosynchronous satellites refueling. Adv. Space Res. 56 (11), 2612–2625.

Zhou, Y., Yan, Y., Huang, X., et al., 2015b. Optimal scheduling of multiple geosynchronous satellites refueling based on a hybrid particle swarm optimizer. Aerosp. Sci. Technol. 47, 125–134.